Chemical Science

ROYAL SOCIETY OF CHEMISTRY

EDGE ARTICLE

View Article Online
View Journal | View Issue

Cite this: *Chem. Sci.*, 2022, **13**, 11215

All publication charges for this article have been paid for by the Royal Society of Chemistry

Received 31st May 2022
Accepted 7th September 2022

DOI: 10.1039/d2sc03054c

rsc.li/chemical-science

Calix[4]pyrrolato gallate: square planar-coordinated gallium(III) and its metal–ligand cooperative reactivity with CO_2 and alcohols†

Lukas M. Sigmund, [a] Eliane Engels,‡[a] Nick Richert‡[a] and Lutz Greb *[b]

Forcing *a priori* tetracoordinate atoms into planar configuration represents a promising concept for enhanced reactivity of p-block element-based systems. Herein, the synthesis, characterization, and reactivity of calix[4]pyrrolato gallates, constituting square planar-coordinated gallium(III) atoms, are reported. Unusual structural constraint-induced Lewis acidity against neutral and anionic donors is disclosed by experiment and rationalized by computations. An energetically balanced dearomatization/rearomatization of a pyrrole unit enables fully reversible metal–ligand cooperative capture of CO_2. While alcohols are found unreactive against the gallates, a rapid and selective OH-bond activation can be triggered upon protonation of the ligand. Secondary ligand–sphere modification adds a new avenue to structurally-constrained complexes that unites functional group tolerance with unconventional reactivity.

Introduction

Steric and electronic effects dictate the tetrahedral arrangement of substituents around tetrasubstituted p-block elements with a complete valence electron octet.[1] While these so-called van't-Hoff–Le-Bel configurations[2,3] are found in most chemical compounds, precise ligand design allowed unique exceptions to this paradigm.[4–13] Most recent additions are the square planar anti-van't-Hoff–Le-Bel cases for aluminum[14,15] and silicon[16] by using the macrocyclic calix[4]pyrrolato ligand (Fig. 1A).[17] While a close-to-planar neutral tetracoordinated gallium atom was recently reported in a pyridine diimine-supported complex,[18] anionic and truly square planar-coordinated gallium, and the reactivity of this compound class, remains elusive.

Planarization results in a distinct alteration of the electronic structure, namely rising the energy of the highest occupied molecular orbital (HOMO) and lowering the energy of the lowest unoccupied molecular orbital (LUMO) (Fig. 1B).[19,20] These features equip the compounds with biphilic properties, ideal for element-ligand cooperative reactivity[21–23] toward various functional groups (Fig. 1A).[14,16,24–26] The potential of gallium–ligand cooperativity (GaLC) was so far exploited with binuclear Ga(II)-species toward unsaturated substrates such as alkynes,[27,28] isocyanates,[29] and others (Fig. 1C).[23,30–33] A few examples of GaLC of mononuclear complexes with amidophenolato[34] or deprotonated β-diketiminato[35] ligands, as well as Berben's pyridine diimine-system[18] are also known to the literature (Fig. 1C).

We herewith report on the synthesis, characterization, and reactivity of two calix[4]pyrrolato gallates(III) (Fig. 1D) and their GaLC reversible addition of CO_2 and protic substrates. They represent the first examples of monoanions with square planar-coordinated gallium(III) atoms and showcase a new direction for reactivity modulation by secondary ligand–sphere modification.

Results and discussion

Reacting the tetrasodium salts of two differently substituted calix[4]pyrrolato ligands[36] with the gallium(III) source tetraphenylphosphonium tetrachloridogallate ($[PPh_4][GaCl_4]$)[37] in 1,2-dimethoxyethane (DME) at room temperature over 3 h resulted in a colorless precipitate (Fig. 2A). After extraction with dichloromethane, pale rose solids were isolated in fair yields (69 and 57%). The ^{1}H NMR spectra of the obtained compounds showed a singlet at around 5.7 ppm and two sets of aliphatic resonances originating from the methyl and ethyl groups, respectively. These characteristics indicate effective solution-phase D_{2d} molecular symmetry, consistent with a square planar environment around the gallium atom. Single crystals obtained from dichloromethane/*n*-pentane mixtures at −40 °C suitable for SCXRD analyses confirmed the NMR spectroscopical data and unveiled the square planar arrangement of the four N-donor sites enclosing the gallium(III) atom (Fig. 2B). The mean Ga–N bond lengths are 193.8(1) and 195.0(1) pm (the data for $[^{Me}\mathbf{1}]^-$ is always given first), which are larger compared to the analogous

[a]*Ruprecht-Karls-Universität Heidelberg, Anorganisch-Chemisches Institut, Im Neuenheimer Feld 270, Heidelberg 69120, Germany*

[b]*Freie Universität Berlin, Anorganische Chemie, Fabeckstraße 34-36, Berlin 14195, Germany. E-mail: lutz.greb@fu-berlin.de*

† Electronic supplementary information (ESI) available. CCDC [2175981–2175983]. For ESI and crystallographic data in CIF or other electronic format see https://doi.org/10.1039/d2sc03054c

‡ These authors contributed equally to this work.

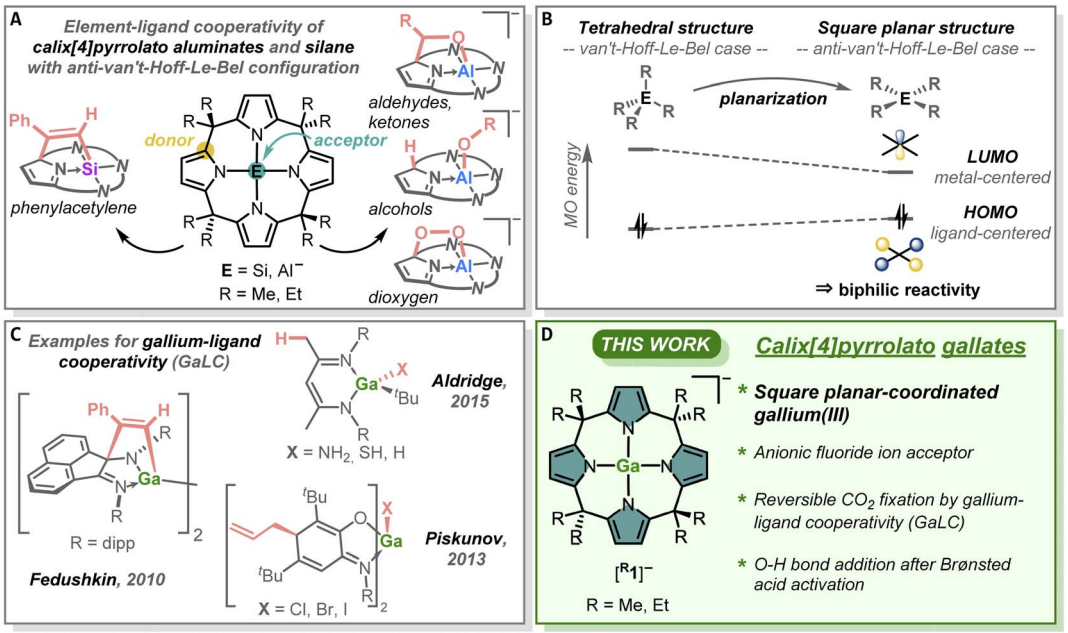

Fig. 1 (a) Element–ligand cooperative reactivity of the aluminum and silicon compounds of the calix[4]pyrrolato ligands. (b) Electronic changes associated with the transformation of the tetrahedral (left) to square planar state (right) for a given tetrasubstituted p-block element. (c) Previous examples for reaction products of gallium–ligand cooperative substrate additions. (d) Calix[4]pyrrolato gallates, described in this work.

aluminum compounds (189.3(2) and 188.3(1) pm).[14,15] The average *cis*- and *trans*-N–Ga–N angles are 90.0(1) and 90.0(1)°, and 178.6(1) and 178.7(1)°, respectively. The τ_4 value of 0.02 for both gallates indicates essentially perfect square planarity.[38] Hence, the calix[4]pyrrolato gallates represent – compared with the neutral gallium pyridine diimine systems (τ_4 = 0.13–0.22) (ref. 18) – the first examples for gallium(III) with ideal square planar, anti-van't-Hoff–Le-Bel configuration.

This structural arrangement was analyzed by various computational techniques (for all computational details see the ESI).† Structural optimization with density functional theory (DFT) confirmed the square planar structure as the energetic global minimum. Constrained structural optimization of $[^{Me}\mathbf{1}]^-$ with the valence angles around the gallium atom fixed to 109.5° gave a conformer 581 kJ mol^{-1} higher in energy as the fully relaxed structure (see Fig. S8 in the ESI).† In comparison, constraining the non-cyclic tetrapyrrolato gallate, which has an effectively tetrahedral ground state, to square planarity costs 166 kJ mol^{-1}.[20] This nicely illustrates the substantial support of the macrocyclic calix[4]pyrrolato ligand and its electronic properties (σ-accepting, π-donating)[39] as being crucial for the experimental realization of this configuration.

The anion $[^{Me}\mathbf{1}]^-$ features an energetically low-lying LUMO (1.48 eV), having its largest coefficient (0.754 within a natural atomic orbital basis) for the 4p$_z$ orbital of the gallium atom (Fig. 2C). In contrast, the HOMO is entirely located in the ligand backbone (Fig. 2C). This agrees with the findings for the corresponding aluminum(III) and silicon(IV) compound and matches early theoretical work from the von Schleyer group.[19] This electronic structure should impart the isolated gallates with biphilic character (*vide infra*). To probe the global Lewis acidity of $[^{Me}\mathbf{1}]^-$, its solution phase (dichloromethane) fluoride ion affinity (FIA$_{solv}$) was computed. It amounts to 149 kJ mol^{-1} ($[^{Et}\mathbf{1}]^-$: 132 kJ mol^{-1}).[40] This value is slightly reduced compared to the analogous aluminate (196 kJ mol^{-1}), though still substantial given the anionic charge state of $[^{Me}\mathbf{1}]^-$. For comparison, the FIA$_{solv}$ value of the tetrahedral tetrapyrrolato gallate is 58 kJ mol^{-1} – corresponding to an increase in Ga–F bond strength of 90 kJ mol^{-1} mainly based on geometric effects!

Following these computational results $[PPh_4][^{Me}\mathbf{1}]$ was reacted with one equivalent of the fluoride ion donor tetrabutylammonium difluorotriphenylsilicate (TBAT) in acetonitrile at room temperature (Fig. 3A). Workup after 4 h afforded an orange solid in 80% yield. Its ^{1}H NMR spectrum showed two doublets for the pyrrolic β-protons and four signals for the methyl groups. Intriguingly, the signal of the *endo*-methyl groups next to the fluoride is split into a doublet (3.1 Hz), indicating through-space fluorine-proton spin–spin coupling. This doublet splitting was also found for the signal of the carbon atom of the respective methyl groups (18.3 Hz). The ^{19}F NMR spectrum contained a resonance at −146 ppm, significantly broadened due to this coupling.[15] In total, this is consistent with the formation of the dianionic $[^{Me}\mathbf{1}\text{-F}]^{2-}$, which was further confirmed by mass spectrometry. These results also agree with the calculated lower FIA$_{solv}$ of fluorotriphenylsilane (85 kJ mol^{-1}) in comparison to the value of $[^{Me}\mathbf{1}]^-$ (see above) and with the overall negative solution-phase Gibbs free reaction energy of −65 kJ mol^{-1} for the fluoride transfer reaction from difluorotriphenylsilicate to $[^{Me}\mathbf{1}]^-$ in acetonitrile. Additional experimental proof for the Lewis acidic reactivity of $[^{Me}\mathbf{1}]^-$ was found when $[PPh_4][^{Me}\mathbf{1}]$ was crystallized from tetrahydrofuran (THF) as solvent.

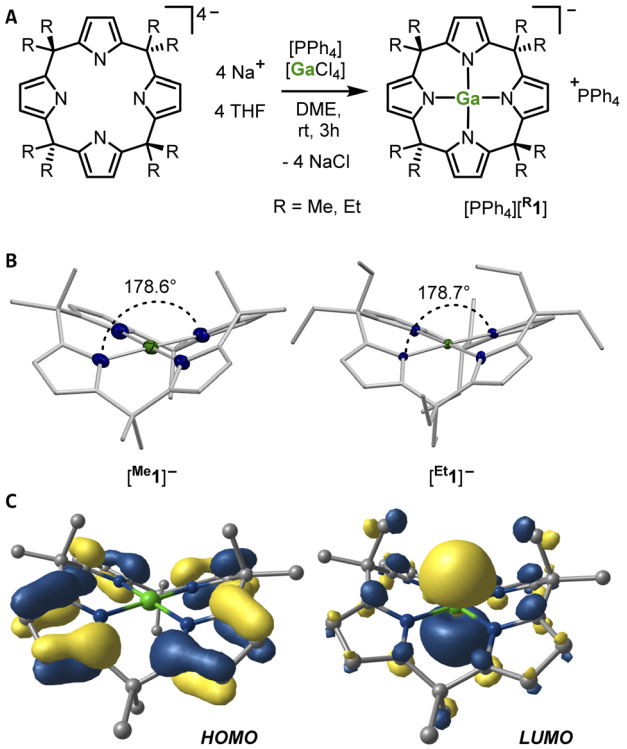

Fig. 2 (a) Synthetic scheme for the preparation of the gallates $[^{Me}\mathbf{1}]^-$ and $[^{Et}\mathbf{1}]^-$ as their $[PPh_4]^+$ salts (DME: 1,2-dimethoxyethane). (b) Solid state molecular structures of $[^{Me}\mathbf{1}]^-$ and $[^{Et}\mathbf{1}]^-$ as determined by SCXRD analyses. The counter cations, cocrystallized solvent molecules, and the hydrogen atoms are not shown. Thermal displacement ellipsoids are presented at a probability level of 50%. Mean Ga–N distances [pm]: $[^{Me}\mathbf{1}]^-$: 193.8(1), $[^{Et}\mathbf{1}]^-$: 195.0(1). Mean *cis*-N–Ga–N angles [°]: $[^{Me}\mathbf{1}]^-$: 90.0(1), $[^{Et}\mathbf{1}]^-$: 90.0(1). Mean *trans*-N–Ga–N angles [°]: $[^{Me}\mathbf{1}]^-$: 178.6(1), $[^{Et}\mathbf{1}]^-$: 178.7(1). CCDC numbers: 2175982, 2175981. (c) Kohn–Sham frontier molecular orbital representations of $[^{Me}\mathbf{1}]^-$. Hydrogen atoms are not shown for clarity.

One THF coordinating to the gallium atom was observed in the solid-state structure with a Ga–O distance of 202.3 pm (Fig. 2B). Interestingly, the computed solution-phase affinity toward THF is low for both gallates ($[^{Me}\mathbf{1}]^-$: 0 kJ mol^{-1}, $[^{Et}\mathbf{1}]^-$: −4 kJ mol^{-1}), allowing for THF removal during the workup of the synthesis of $[PPh_4][^{Me}\mathbf{1}]$ and $[PPh_4][^{Et}\mathbf{1}]$, respectively.

Having established the Lewis acidity of the gallates by computations and experiment, it was tested whether their properties arising from the square planar-coordinated Ga(III) atoms serve to facilitate reactions with other substrate molecules. The analogous calix[4]pyrrolato aluminate showed manifold reactivity with carbonyl-containing compounds (see Fig. 1A);[25] so we reacted $[PPh_4][^{Me}\mathbf{1}]$ and $[PPh_4][^{Et}\mathbf{1}]$ with carbon dioxide.

After exposing both gallates dissolved in dichloromethane-d_2 to 5 bar of CO_2 at room temperature, the solutions turned intensively yellow within several hours. This color change indicates the dearomatization of one pyrrole moiety (marked with an asterisk in the following formulae). The ^{1}H NMR spectra showed the clean emergence of a new C_1 symmetric species, which was unambiguously identified as the gallium–ligand

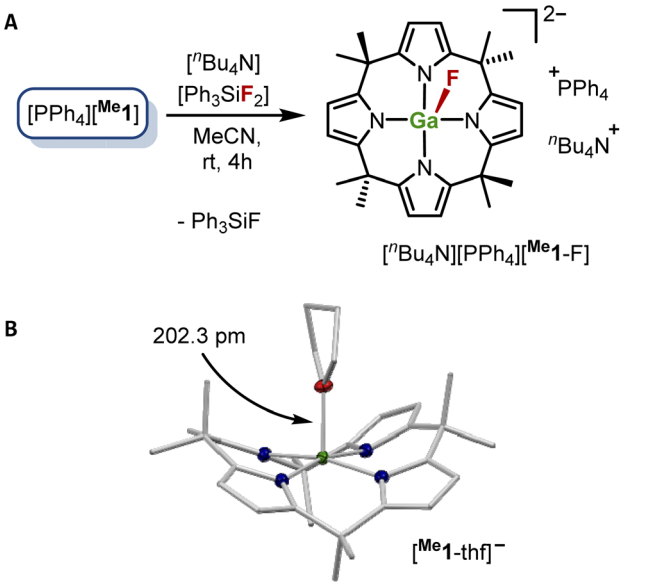

Fig. 3 Lewis acidic reactivity of $[^{Me}\mathbf{1}]^-$ as demonstrated (a) by the reaction of $[PPh_4][^{Me}\mathbf{1}]$ with tetrabutylammonium difluorotriphenylsilicate (TBAT) and (b) by the solid-state structures as determined by SCXRD analysis of $[PPh_4][^{Me}\mathbf{1}]$ crystallized from THF as solvent. Thermal displacement ellipsoids are shown at a probability level of 50%. Selected bond lengths [pm]: Ga–O: 202.30(8), mean Ga–N: 199.32(5). Selected bond angles [°]: mean *cis*-N–Ga–N angle: 89.21(2), mean *trans*-N–Ga–N angle: 166.5(1), mean O–Ga–N*X* (*X* = 1, 2, 3, 4) angle: 96.8(1). CCDC number: 2175983.

cooperative addition product of CO_2 to $[^{Me}\mathbf{1}]^-$ and $[^{Et}\mathbf{1}]^-$, respectively (Fig. 4, see the ESI for details).† Interestingly, the conversion to $[^{R}\mathbf{1}^*\text{-}CO_2]^-$ was found almost quantitative for the methyl case (96%), whereas a 2 : 1 ratio of starting material to addition product was observed for the ethyl gallate under the chosen reaction conditions. The Gibbs free activation energy for the addition reaction of CO_2 to $[^{Me}\mathbf{1}]^-$ was calculated to $\Delta G_r^{\ddagger} =$ 90 kJ mol^{-1}, and the overall Gibbs free reaction energy to $\Delta G_r =$ 6 kJ mol^{-1}, which conforms with the experimental observations. Further, the computational simulations reproduced the decreased binding strength of CO_2 to $[^{Et}\mathbf{1}]^-$ ($\Delta G_r =$ 18 kJ mol^{-1}). This may be rationalized by the slightly decreased Lewis acidity on the FIA_{solv} scale of the gallium atom in $[^{Et}\mathbf{1}]^-$ (see above) as well as by a larger stabilization of $[^{Me}\mathbf{1}^*\text{-}CO_2]^-$ in a dichloromethane solution as found by COSMO-RS[41–43] calculations (see Chapter S11 in the ESI).†

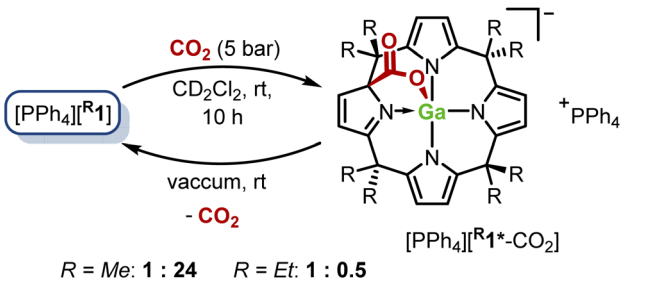

Fig. 4 Reactivity of $[PPh_4][^{R}\mathbf{1}]$ with CO_2.

In agreement with these thermoneutral computed values, the application of reduced pressure to solutions of $[PPh_4][^{R}\mathbf{1}^{*}\text{-}CO_2]$ over several hours at room temperature resulted in the quantitative removal of CO_2 from the systems and in the selective reformation of $[^{R}\mathbf{1}]^{-}$ (see Fig. S1 and S2 in the ESI).† Element-ligand cooperative (ELC) binding of CO_2 is a widely studied reaction with various transition metals[44–50] and p-block elements[51–59] and was also investigated in small molecule contexts other than ELC.[35,60–66] To the best of our knowledge, the described reaction represents the first example for reversible CO_2 fixation by a gallium(III) platform. This is achieved by the balanced energetics in dearomatization/rearomatization of one of the pyrrole rings of the calix[4]pyrrolato ligand.

We next turned our attention to protic substrates, namely alcohols, as their ready activation by the calix[4]pyrrolato aluminate was already noticed by our group.[24] Upon reacting one equivalent of ^{i}PrOH with $[PPh_4][^{Me}\mathbf{1}]$ and $[PPh_4][^{Et}\mathbf{1}]$, respectively, no reaction occurred, contrasting the behavior of the corresponding aluminates, *i.e.*, the formation of an oxygen–element bond with the proton being transferred to the 2-position of one of the pyrrole rings (Fig. 5B, left part). We reasoned that protonation of the ligand backbone might serve as a powerful strategy for second-sphere reactivity modulation in structurally constrained complexes. Such tactics are well-known in an alternative context,[67] for example, applied by the Corey group in enantioselective Diels–Alder catalysis.[68–70] To probe this hypothesis computationally, the α-pyrrole protonated, neutral $[H\text{-}^{Me}\mathbf{1}^{*}]$ was optimized by DFT and its electronic structure was examined. The HOMO is now concentrated almost exclusively in the pyrrole unit opposite the protonation site, which itself is hosting the LUMO (Fig. 5A). The LUMO+1 resembles the former LUMO (cf. Fig. 2C) with the dominant contribution of the $4p_z$ orbital of the gallium atom. The calculated solution phase FIA of $[H\text{-}^{Me}\mathbf{1}^{*}]$, which was 149 kJ mol^{-1} for $[^{Me}\mathbf{1}]^{-}$, is now boosted to 191 kJ mol^{-1}, pointing to an augmented Lewis acidity.

Motivated by these computational results $[PPh_4][^{Me}\mathbf{1}]$ and $[PPh_4][^{Et}\mathbf{1}]$ were treated with bis(trifluoromethyl)sulfonimide ($HNTf_2$) in dichloromethane-d_2 as solvent. The ^{1}H NMR spectra of the reaction mixtures showed an unselective product mixture. Computations disclosed a potential decomposition channel initiated after the formation of $[H\text{-}^{Me}\mathbf{1}^{*}]$ by the cleavage of the exopyrrolic C–C bond originating from the proton-bearing carbon atom of the dearomatized pyrrole ring (see Chapter S8 in the ESI for details).† However, a selective transformation was observed when THF-d_8 was used as solvent. The ^{1}H NMR data revealed the dearomatization of one of the pyrrole rings, besides a slightly broadened singlet resonance at 5.02 ppm, assigned to the new proton in the 2-position of the dearomatized pyrrole ring. Apparently, the Lewis basic properties of THF suppress the undesired pathway mentioned above. Indeed, remodeling the C–C bond cleavage transition state in the presence of an explicit THF molecule coordinating to Ga in $[H\text{-}^{Me}\mathbf{1}^{*}]$, resulted in a significant increase in Gibbs free activation energy of 64 kJ mol^{-1} (see the ESI for details).† When repeating the reaction with $HNTf_2$ in a mixture of dichloromethane-d_2 and diethyl ether (2 : 1 % vol), the same ^{1}H NMR characteristics were found, supporting the Lewis base stabilization rationale.

Subsequently, the reaction with ^{i}PrOH was repeated with the *in situ* generated $[H\text{-}^{Me}\mathbf{1}^{*}]\cdot Et_2O$ in the dichloromethane/diethyl ether mixture. After stirring at room temperature for 1 min, removing the solvent, and extracting with *n*-pentane/diethyl ether (4 : 1 % vol), a pale-yellow solid was isolated in 72% yield. Its ^{1}H NMR spectrum showed the formation of a symmetric species with two dearomatized pyrrole rings due to protonation at the 2-positions and an isopropyl group with shifted signals compared to free ^{i}PrOH. These features align

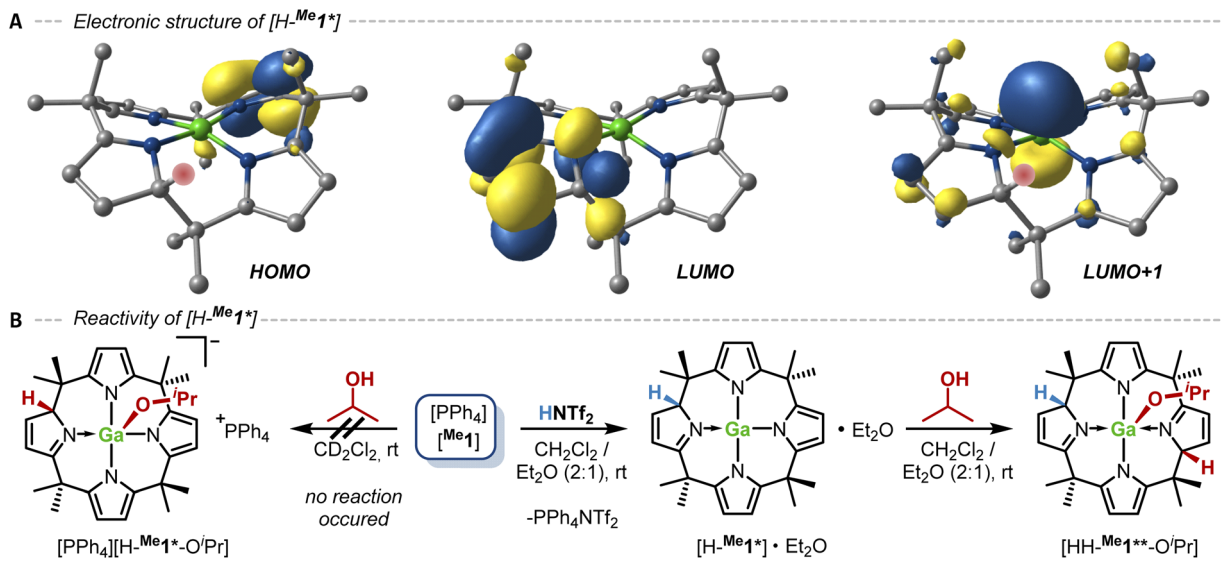

Fig. 5 (a) Kohn–Sham frontier molecular orbital representations of $[H\text{-}^{Me}\mathbf{1}^{*}]$. Hydrogen atoms, except for the one inducing dearomatization of one pyrrole ring, are not shown for clarity. (b) Reactivity of isopropanol with $[PPh_4][^{Me}\mathbf{1}]$ (left part) and $[H\text{-}^{Me}\mathbf{1}^{*}]\cdot Et_2O$ (right part), *in situ* generated by treatment of $[PPh_4][^{Me}\mathbf{1}]$ with bis(trifluoromethyl)sulfonimide ($HNTf_2$).

with the formation of the neutral O–H bond addition product [HH-^{Me}**1****-O^{i}Pr] by gallium–ligand cooperativity (Fig. 5B, right part). Hence, whereas [^{Me}**1**]$^{-}$ itself is not capable of splitting the O–H bond by GaLC, the protonated, neutral [H-^{Me}**1***]·Et_2O instantaneously adds ^{i}PrOH. It confirms the hypothesis that the reactivity of [^{Me}**1**]$^{-}$ can be enhanced by protonation of the ligand backbone.

Conclusions

In conclusion, we report on the synthesis, characterization, and reactivity of two calix[4]pyrrolato gallates(III), which feature a nearly ideal square planar coordination environment around their gallium atoms. Structural constraint empowers Lewis acidic reactivity by p_z-type LUMO-lowering, primarily at gallium. This was experimentally proven with donors like THF or fluoride anions, opposing Coulomb repulsion in the latter case. Reversible metal–ligand cooperative addition of CO_2 is achieved *via* the dearomatization/rearomatization of one of the pyrrole units. The associated equilibrium can be fine-tuned by substituent variation in the ligand backbone. Isopropanol as a model for protic substrates did not react with the gallates in the first place, but a rapid reaction was triggered upon activation with a Brønsted acid. Overall, the reactivity of the square-planar gallate is inherently lower compared to the corresponding aluminate – in line with related reports.[18] This observation can be explained by the lower global Lewis acidity of gallium. Notably, second-sphere ligand modification by protonation is identified as a powerful handle to circumvent this limitation. This strategy will account for a more general approach to increase the reactivity of p-block element complexes of the calix[4]pyrrolato ligand and broadens the substrate scope for more challenging bond activation reactions.

Data availability

Crystallographic data has been deposited at the CCDC under 2175981–2175983. Further datasets supporting this article have been uploaded as part of the ESI.†

Author contributions

L. G. and L. M. S. devised the project and designed the experiments. L. M. S carried out the calculations, did the experimental work together with E. E. and N. R., and analyzed the data. L. G. and L. M. S. wrote the manuscript.

Conflicts of interest

There are no conflicts to declare.

Acknowledgements

Financial support for this project was provided by the European Research Council (ERC) under the European Union's Horizon 2020 research and innovation program (grant agreement no 948708). L. M. S. is grateful to the "Studienstiftung des deutschen Volkes" for a scholarship. For computational resources, we thank the state of Baden-Württemberg for the bwHPC system (JUSTUS 2). E. Filbeck and H. Ruppert are acknowledged for carrying out the SCXRD measurements and Dr D. Hartmann for assistance with structure refinement and finalization.

References

1 T. A. Albright, J. K. Burdett and M.-H. Whangbo, *Orbital interactions in chemistry*, Wiley, Hoboken, NJ, 2013.
2 J. H. van't Hoff, *Arch. Neerl. Sci. Exactes Nat.*, 1874, **9**, 445–454.
3 J. A. Le Bel, *Bull. Soc. Chim. Fr.*, 1874, **22**, 337–347.
4 J. B. Collins, J. D. Dill, E. D. Jemmis, Y. Apeloig, P. v. R. Schleyer, R. Seeger and J. A. Pople, *J. Am. Chem. Soc.*, 1976, **98**, 5419–5427.
5 E.-U. Würthwein and P. v. R. Schleyer, *Angew. Chem., Int. Ed.*, 1979, **18**, 553–554.
6 A. I. Boldyrev, P. v. R. Schleyer and R. Keese, *Mendeleev Commun.*, 1992, **2**, 93–95.
7 M. Menzel, D. Steiner, H.-J. Winkler, D. Schweikart, S. Mehle, S. Fau, G. Frenking, W. Massa and A. Berndt, *Angew. Chem., Int. Ed.*, 1995, **34**, 327–329.
8 D. Röttger and G. Erker, *Angew. Chem., Int. Ed.*, 1997, **36**, 812–827.
9 M. Driess, J. Aust, K. Merz and C. van Wüllen, *Angew. Chem., Int. Ed.*, 1999, **38**, 3677–3680.
10 D. W. Stephan, *Angew. Chem., Int. Ed.*, 2000, **39**, 501–502.
11 R. Keese, *Chem. Rev.*, 2006, **106**, 4787–4808.
12 E. J. Thompson, T. W. Myers and L. A. Berben, *Angew. Chem., Int. Ed.*, 2014, **53**, 14132–14134.
13 L.-M. Yang, E. Ganz, Z. Chen, Z.-X. Wang and P. V. R. Schleyer, *Angew. Chem., Int. Ed.*, 2015, **54**, 9468–9501.
14 F. Ebner, P. Mainik and L. Greb, *Chem.–Eur. J.*, 2021, **27**, 5120–5124.
15 F. Ebner, H. Wadepohl and L. Greb, *J. Am. Chem. Soc.*, 2019, **141**, 18009–18012.
16 F. Ebner and L. Greb, *Chem*, 2021, **7**, 2151–2159.
17 H. Ruppert, L. M. Sigmund and L. Greb, *Chem. Commun.*, 2021, **57**, 11751–11763.
18 T. M. Bass, C. R. Carr, T. J. Sherbow, J. C. Fettinger and L. A. Berben, *Inorg. Chem.*, 2020, **59**, 13517–13523.
19 M. B. Krogh-Jespersen, J. Chandrasekhar, E.-U. Würthwein, J. B. Collins and P. v. R. Schleyer, *J. Am. Chem. Soc.*, 1980, **102**, 2263–2268.
20 L. M. Sigmund, R. Maier and L. Greb, *Chem. Sci.*, 2022, **13**, 510–521.
21 C. Gunanathan and D. Milstein, *Acc. Chem. Res.*, 2011, **44**, 588–602.
22 J. R. Khusnutdinova and D. Milstein, *Angew. Chem., Int. Ed.*, 2015, **54**, 12236–12273.
23 L. Greb, F. Ebner, Y. Ginzburg and L. M. Sigmund, *Eur. J. Inorg. Chem.*, 2020, **2020**, 3030–3047.
24 L. M. Sigmund and L. Greb, *Chem. Sci.*, 2020, **11**, 9611–9616.
25 F. Ebner, L. M. Sigmund and L. Greb, *Angew. Chem., Int. Ed.*, 2020, **59**, 17118–17124.

26 L. M. Sigmund, C. Ehlert, M. Enders, J. Graf, G. Gryn'ova and L. Greb, *Angew. Chem., Int. Ed.*, 2021, **60**, 15632–15640.
27 I. L. Fedushkin, A. S. Nikipelov and K. A. Lyssenko, *J. Am. Chem. Soc.*, 2010, **132**, 7874–7875.
28 I. L. Fedushkin, A. S. Nikipelov, A. G. Morozov, A. A. Skatova, A. V. Cherkasov and G. A. Abakumov, *Chem.–Eur. J.*, 2012, **18**, 255–266.
29 V. A. Dodonov, W. Chen, Y. Zhao, A. A. Skatova, P. W. Roesky, B. Wu, X.-J. Yang and I. L. Fedushkin, *Chem.–Eur. J.*, 2019, **25**, 8259–8267.
30 I. L. Fedushkin, V. A. Dodonov, A. A. Skatova, V. G. Sokolov, A. V. Piskunov and G. K. Fukin, *Chem.–Eur. J.*, 2018, **24**, 1877–1889.
31 W. Zhang, V. A. Dodonov, W. Chen, Y. Zhao, A. A. Skatova, I. L. Fedushkin, P. W. Roesky, B. Wu and X.-J. Yang, *Chem.–Eur. J.*, 2018, **24**, 14994–15002.
32 D. A. Razborov, A. N. Lukoyanov, M. V. Moskalev, E. V. Baranov and I. L. Fedyushkin, *Russ. J. Coord. Chem.*, 2018, **44**, 380–387.
33 I. L. Fedushkin, A. N. Lukoyanov, S. Y. Ketkov, M. Hummert and H. Schumann, *Chem.–Eur. J.*, 2007, **13**, 7050–7056.
34 A. V. Piskunov, I. V. Ershova, G. K. Fukin and A. S. Shavyrin, *Inorg. Chem. Commun.*, 2013, **38**, 127–130.
35 J. A. B. Abdalla, I. M. Riddlestone, R. Tirfoin and S. Aldridge, *Angew. Chem., Int. Ed.*, 2015, **54**, 5098–5102.
36 W. J. Transue, Y. Dai, M.-L. Y. Riu, G. Wu and C. C. Cummins, *Inorg. Chem.*, 2021, **60**, 9254–9258.
37 L. E. Maelia and S. A. Koch, *Inorg. Chem.*, 1986, **25**, 1896–1904.
38 L. Yang, D. R. Powell and R. P. Houser, *Dalton Trans.*, 2007, 955–964.
39 W. P. Ozimiński and J. C. Dobrowolski, *J. Phys. Org. Chem.*, 2009, **22**, 769–778.
40 P. Erdmann, J. Leitner, J. Schwarz and L. Greb, *ChemPhysChem*, 2020, **21**, 987–994.
41 A. Klamt, *J. Phys. Chem.*, 1995, **99**, 2224–2235.
42 A. Klamt, V. Jonas, T. Bürger and J. C. W. Lohrenz, *J. Phys. Chem. A*, 1998, **102**, 5074–5085.
43 A. Klamt, *COSMO-RS From Quantum Chemistry to Fluid Phase Thermodynamics and Drug Design*, Elsevier Science Amsterdam, 2005.
44 M. Vogt, M. Gargir, M. A. Iron, Y. Diskin-Posner, Y. Ben-David and D. Milstein, *Chem.–Eur. J.*, 2012, **18**, 9194–9197.
45 M. Vogt, A. Nerush, Y. Diskin-Posner, Y. Ben-David and D. Milstein, *Chem. Sci.*, 2014, **5**, 2043–2051.
46 D. Sieh, D. C. Lacy, J. C. Peters and C. P. Kubiak, *Chem.–Eur. J.*, 2015, **21**, 8497–8503.
47 R. Stichauer, A. Helmers, J. Bremer, M. Rohdenburg, A. Wark, E. Lork and M. Vogt, *Organometallics*, 2017, **36**, 839–848.
48 M. Feller, E. Ben-Ari, Y. Diskin-Posner and D. Milstein, *J. Coord. Chem.*, 2018, **71**, 1679–1689.
49 I. Heuermann, B. Heitmann, R. Stichauer, D. Duvinage and M. Vogt, *Organometallics*, 2019, **38**, 1787–1799.
50 A. Kumar, P. Daw, N. A. Espinosa-Jalapa, G. Leitus, L. J. W. Shimon, Y. Ben-David and D. Milstein, *Dalton Trans.*, 2019, **48**, 14580–14584.
51 M. A. Dureen and D. W. Stephan, *J. Am. Chem. Soc.*, 2010, **132**, 13559–13568.
52 D. A. Dickie, E. N. Coker and R. A. Kemp, *Inorg. Chem.*, 2011, **50**, 11288–11290.
53 E. Theuergarten, J. Schlösser, D. Schlüns, M. Freytag, C. G. Daniliuc, P. G. Jones and M. Tamm, *Dalton Trans.*, 2012, **41**, 9101–9110.
54 L. J. Hounjet, C. B. Caputo and D. W. Stephan, *Angew. Chem., Int. Ed.*, 2012, **51**, 4714–4717.
55 M.-A. Courtemanche, J. Larouche, M.-A. Légaré, W. Bi, L. Maron and F.-G. Fontaine, *Organometallics*, 2013, **32**, 6804–6811.
56 D. A. Dickie and R. A. Kemp, *Organometallics*, 2014, **33**, 6511–6518.
57 D. A. Dickie, M. T. Barker, M. A. Land, K. E. Hughes, J. A. C. Clyburne and R. A. Kemp, *Inorg. Chem.*, 2015, **54**, 11121–11126.
58 N. von Wolff, G. Lefèvre, J. C. Berthet, P. Thuéry and T. Cantat, *ACS Catal.*, 2016, **6**, 4526–4535.
59 T. S. Koptseva, V. G. Sokolov, S. Y. Ketkov, E. A. Rychagova, A. V. Cherkasov, A. A. Skatova and I. L. Fedushkin, *Chem.–Eur. J.*, 2021, **27**, 5745–5753.
60 C. M. Mömming, E. Otten, G. Kehr, R. Fröhlich, S. Grimme, D. W. Stephan and G. Erker, *Chem., Int. Ed.*, 2009, **48**, 6643–6646.
61 F. Buß, P. Mehlmann, C. Mück-Lichtenfeld, K. Bergander and F. Dielmann, *J. Am. Chem. Soc.*, 2016, **138**, 1840–1843.
62 L. F. B. Wilm, T. Eder, C. Mück-Lichtenfeld, P. Mehlmann, M. Wünsche, F. Buß and F. Dielmann, *Green Chem.*, 2019, **21**, 640–648.
63 Y. Yang, L. Yan, Q. Xie, Q. Liang and D. Song, *Org. Biomol. Chem.*, 2017, **15**, 2240–2245.
64 A. Caise, J. Hicks, M. Ángeles Fuentes, J. M. Goicoechea and S. Aldridge, *Chem.–Eur. J.*, 2021, **27**, 2138–2148.
65 M. Xu, A. R. Jupp and D. W. Stephan, *Angew. Chem., Int. Ed.*, 2017, **56**, 14277–14281.
66 J. N. Gayton, Q. Li, L. Sanders, R. R. Rodrigues, G. Hill and J. H. Delcamp, *ACS Omega*, 2020, **5**, 11687–11694.
67 H. Yamamoto and K. Futatsugi, *Angew. Chem., Int. Ed.*, 2005, **44**, 1924–1942.
68 E. J. Corey, T. Shibata and T. W. Lee, *J. Am. Chem. Soc.*, 2002, **124**, 3808–3809.
69 D. H. Ryu and E. J. Corey, *J. Am. Chem. Soc.*, 2003, **125**, 6388–6390.
70 D. H. Ryu, T. W. Lee and E. J. Corey, *J. Am. Chem. Soc.*, 2002, **124**, 9992–9993.